Molecular Therapy
Oncolytics
Original Article

AMERICAN SOCIETY of GENE & CELL THERAPY

An Engineered AAV6-Based Vaccine Induces High Cytolytic Anti-Tumor Activity by Directly Targeting DCs and Improves Ag Presentation

Karina Krotova,[1] Andrew Day,[1] and George Aslanidi[1]

[1]The Hormel Institute, University of Minnesota, Austin, MN, USA

We have previously shown that an AAV6-based vaccine generates high levels of antigen-specific CD8$^+$ T cells. Further modifications described here led to significantly increased levels of antigen-specific CD8$^+$ and CD4$^+$ T cells, enhanced formation of memory cells, and superior antigen-specific killing capacity in a murine model. By tracking reporter-gene-positive dendritic cells, we showed that they were directly targeted with modified AAV6 *in vivo*. Our vaccine's anti-cancer potential was evaluated with the antigen ovalbumin against a B16F10 melanoma cell line stably expressing ovalbumin. The vaccination showed superior protection in a murine model of metastatic melanoma. The vaccination significantly delayed solid tumor growth but did not completely prevent tumor development. We show that tumors in immunized mice escaped vaccine-induced killing by losing ovalbumin expression. The vaccine induced massive tumor infiltration with NK and CD8$^+$ T cells with upregulated PD-1 expression. Thus, a vaccination of a combination of anti-PD-1 antibodies demonstrated significant improvement in the treatment efficacy. To summarize, we showed that a bioengineered AAV6-based vaccine elicits strong and long-lasting cellular and humoral responses against an encoded antigen. To increase AAV vaccine efficiency and mitigate tumor escape through antigen loss, we intended to target several antigens in combination with treatments targeting the tumor microenvironment.

INTRODUCTION

Anti-cancer vaccines are a type of immunotherapy aimed to induce cell-mediated host immunity, so that cytotoxic T lymphocytes (CTLs) are activated to identify and destroy cancer cells. In early clinical trials, cancer vaccines as monotherapy showed moderate clinical response compared to more successful CTL-based immunotherapies such as adoptive tumor infiltrating lymphocytes-cell transfer or chimeric antigen receptors T cells.[1,2] Major obstacles in vaccine efficiency included suboptimal vaccine design as well as immunosuppression of generated CTLs by the tumor microenvironment (TME). However, the production and cost advantages, the safety profile, and the compatibility with other immunomodulatory and standard treatments that vaccination offers warranted the search for new approaches to develop an effective cancer vaccine.[3–5]

Therapeutic vaccines need a rational design that results in concentrated antigen (Ag) delivery to dendritic cells (DCs) and appropriate DC activation, which, in turn, drives both CD4$^+$ and CD8$^+$ T cell responses and creates memory cells.[6] Adeno-associated virus (AAV)-based vectors have several beneficial features for cancer vaccine development. First, AAV has been shown to be a safe and efficient vector in a number of clinical studies;[7–11] recently, two treatments for congenital blindness and spinal muscular atrophy have been approved by the US Food and Drug Administration (FDA).[12] Second, recent data obtained from clinical studies changed the paradigm about low AAV immunogenicity.[13] Several natural and engineered AAV serotypes can induce strong cellular immune responses against an encoded transgene, an important feature needed for vaccine development, and showed protective anti-cancer immune response in mouse animal models.[14–19] Third, much research was done to understand the interaction of AAV with DCs and improve AAV infectivity by modifying the viral capsid to overcome intracellular obstacles such as proteasomal degradation[20,21] and vector uncoating.[22]

DCs, as professional antigen-presenting cells (APCs), can present Ags either by direct presentation of a gene delivered into DCs or by cross-presentation of Ags released from transduced tissue and taken up by un-transfected DCs. Both pathways can be targeted by vaccines, but direct Ag delivery is preferred, since transduced DCs play a predominant role in the presentation of Ags to CD8$^+$ T cells.[23] We chose AAV6 as a vector based on its ability to directly infect DCs *in vitro* and to generate cytotoxic effector and memory T cells *in vivo*.[18,19,21,24,25] Another prerequisite for proper T cell priming by DCs is the maturation of DCs after loading with an Ag, which requires additional activation signals.[14] Microbial vectors, like *L. monocytogenes*[26] or vaccinia virus,[27] themselves can serve as sources of immune danger signals[28] or pathogen-associated molecular patterns[29] that aid in DC maturation. AAV is also recognized by cells as a viral entity, but inflammation induced by AAV is mild and

Received 23 September 2019; accepted 1 October 2019;
https://doi.org/10.1016/j.omto.2019.10.001.

Correspondence: George Aslanidi, PhD, The Hormel Institute, University of Minnesota, 801 16th Avenue NE, Austin, MN 55912, USA.
E-mail: gaslanid@umn.edu

temporal compared to that induced by other commonly used vectors such as adenovirus, which induces high levels of systemic inflammation.[30]

In our previous studies, we have showed that the optimization of AAV6 capsid dramatically improves transduction efficiency of human monocyte-derived DCs[21] and mouse CD34$^+$-cell-derived DCs and also stimulates the protective immune response in the mouse model of prostate cancer.[25] In recent studies, we optimized the design of expression cassette and observed a significant increase in antigen-specific CD8$^+$ and CD4$^+$ T cells as well as improved formation of memory cells and, consequently, long-term killing ability of these effector cells. In this article, we also focused on the mechanism of our AAV-based vaccine function, effector cell interaction with tumor microenvironment and changes induced by vaccination in immune cell populations in tumor. The characterization of changes in tumor microenvironment will provide the rational for future potential clinical AAV-based vaccine application, particularly in combination with common and emerging treatments. We used ovalbumin (Ova) as a well-characterized model antigen that provided a reliable opportunity to identify and follow Ag-specific T cells in C57BL/6 mouse. The therapeutic potential of our novel optimized vaccine was analyzed in B16F10 melanoma cells stably expressing Ova (B16/Ova). Additionally, we have shown that vaccine can overcome the tolerance of the immune system against endogenous self-proteins, and an AAV-based vaccine successfully generates cytotoxic T cell response against two melanoma self-antigens, tyrosinase (Tyr) and premelanosome protein (gp100).[31–33]

RESULTS

AAV6 Capsid Optimization to Improve Ag Presentation to CD8$^+$ T Cells

The ability of AAV serotype 6 to target APCs was demonstrated previously.[21,34,35] In addition, the modifications of residues on the AAV capsid, critical for the interaction of the virus with cellular components during infection, can increase the transduction efficiency of AAV vectors in different tissues and cells.[36–39] As a vaccine vector, we used AAV6 with the substitution of serine at position 663 for valine (S663V) on the capsid that improves AAV intracellular trafficking and nuclear translocation.[21] As a model antigen, we used Ova under a strong cytomegalovirus (CMV) promoter, which was packed as a self-complimentary (sc) vector to overcome the rate-limiting step of viral second-strand DNA synthesis necessary for single-strand (ss) AAV,[40] and shown to be more effective in DCs.[34,41] An additional advantage of using scAAV compared to ssAAV for vaccination studies is an induction of a stronger adaptive immune response, because it is recognized as viral DNA by Toll-like receptor (TLR)-9.[42] Vectors were administrated to mice as a single intramuscular (intramuscular) injection, and the levels of Ova-specific CD8$^+$ T cells were detected in the mouse blood by staining with major histocompatibility complex (MHC) class I Ova-specific tetramers ($Ova_{257–264}$ [SIINFEKL] tetramers). The modified capsid (663-Ova) resulted in significantly higher levels of Ova-specific CD8$^+$ T cells compared to wild-type (WT) AAV6 (WT-Ova) (Figure 1A). To estimate functional activity of generated cells, splenocytes were isolated 3 weeks after immunization, and the production of interferon γ (IFNγ) in response to stimulation with MHC class I peptide $Ova_{257–264}$ was analyzed by the enzyme-linked immunospot (ELISPOT) assay. Splenocytes from animals immunized with 663-Ova consistently had high levels of IFNγ-producing cells. In contrast, animals immunized with WT-AAV6 displayed vast inconsistency (Figure 1B). We also analyzed the ability of the vaccine to generate a humoral response against Ags. AAV vectors are known for their ability to elicit high titers of antibodies against a transgene.[24,43] These antibodies, if their cognate epitopes are expressed on the tumor cell surface, could be a complimentary part of an anti-cancer treatment by opsonizing tumor cells and, consequently, facilitating tumor destruction by innate immune cells.[44,45] Both vaccines showed high titers of Ova-specific antibodies 3 weeks after immunization (Figure 1C). In summary, these data identify our AAV6 mutant as a suitable vector for tumor vaccine, as a single intramuscular injection is able to generate both cellular and humoral responses. All following experiments were performed with this capsid modified AAV6-S663V (663) vector.

AAV6-S663V Directly Targets DCs *In Vivo*

Naive CD8$^+$ T cells are activated by the presence of peptide-MHC class I complexes on the surface of APCs. MHC class I molecules typically present peptides derived from endogenous Ags. Loading of exogenous Ags on class I molecules, e.g., in cross-priming, sometimes occurs but to a lesser extent.[46,47] In addition, cross-presentation usually occurs on a specialized class of DCs.[48]

We and others have shown previously that AAV6 and its modifications are able to efficiently deliver Ags to human and murine DCs *in vitro*.[21,25,34,35] To show direct delivery of antigens to DCs *in vivo*, mice were injected with AAV6-663-expressing GFP under a CMV promoter in the biceps femoris muscle, and 4 days later, DCs from draining lymph nodes were isolated by CD11c-positive selection columns. Flow cytometry analysis showed that, after immunization, up to 10% of draining lymph node DCs (CD11c$^+$, MHC II$^+$) were GFP positive (Figure 1D). Analysis of isolated DCs under a fluorescent microscope confirmed the presence of GFP-expressing DCs in draining lymph nodes of AAV-immunized animals (Figure 1E). Together, these data validated that our vaccine efficiently and directly delivers Ags to DCs.

Fusion of Ag with Trafficking Signals of MHC Class I Molecule Increases the Number of Ag-Specific CD4$^+$ and CD8$^+$ T Cells

Next, we addressed the presentation of Ags delivered by AAV vectors on the MHC class II molecule. In general, the presentation of antigenic peptides by MHC class II molecules to CD4$^+$ T cells dramatically increases the potency of anti-tumor vaccines.[49] Though CD8$^+$ T cells are considered the major cytotoxic entity against tumor, CD4$^+$ T cells orchestrate and enhance tumor destruction through CD8$^+$-dependent and -independent pathways.[50–52] The assistance provided by cognate CD4$^+$ T cells during priming increases clonal expansion of tumor-specific CD8$^+$ T cells in secondary lymphoid tissue; these cells show greater resistance to cell death upon secondary encounter with Ags and develop functional memory cells.[53–57] Several

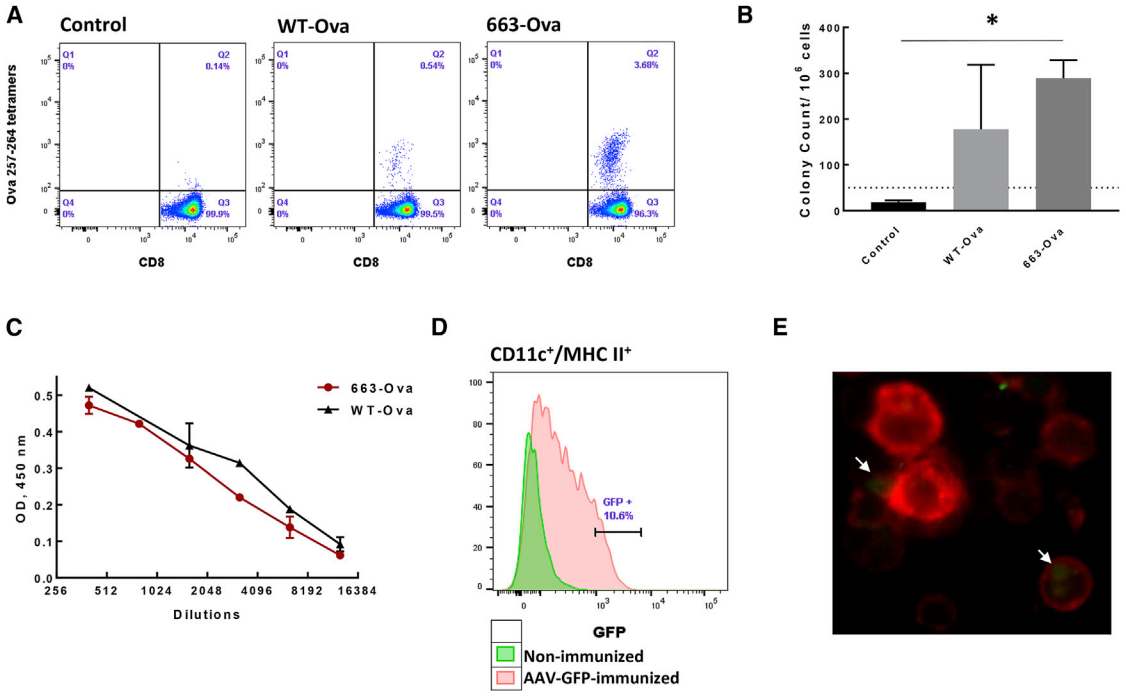

Figure 1. AAV6-Based Vaccines Induce Strong Cellular and Humoral Response against Antigen by Targeting DC *In Vivo*

(A) Optimization of the AAV6 capsid increases proportion of $Ova_{257–264}$-tet$^+$ cells. The levels of $Ova_{257–264}$-tet$^+$ cells were measured in the blood of mice by using Ova MHC class I tetramers 14 days after i.m. immunization with different AAV6-Ova constructs. (B) The activity of Ova-specific CD8$^+$ T cells was estimated by IFNγ production. Splenocytes were isolated 3 weeks after immunization and re-stimulated with $Ova_{257–264}$ peptide (SIINFEKL) to analyze IFNγ production by ELISPOT assay. (C) Vaccination induces strong humoral response. Ova-specific antibodies were measured in serial dilutions of mouse plasma 3 weeks after immunization. All values were normalized to background, which was determined as values from plasma of naive mice. Data are representative of experiments repeated 3 times with similar results. OD, optical density. (D and E) AAV6/CMV-GFP administered in an i.m. injection targets DCs *in vivo*. Briefly, 4 days after i.m. injection, (D) DCs were isolated from drained lymph nodes by a CD11c$^+$ magnetic beads kit (BioLegend) and analyzed by FACS, or (E) cells were labeled with MHC class II– APC antibodies (red channel), and the presence of GFP expression was analyzed by fluorescence microscopy. White arrows indicate DCs expressing GFP. * $p < 0.05$. ** $p < 0.01$.

approaches were described to help endogenously expressed Ags to be processed in the endosomal/lysosomal compartment, which allows newly formed antigenic peptides to complex with MHC class II molecules.[58–64] In general, these strategies fuse Ags with trafficking signals of lysosomal or endosomal proteins. To increase the efficacy of vaccine, we flanked the Ova gene with trafficking signals of MHC class I molecule, as originally described by Kreiter et al.[62] This strategy was based on the observation that MHC class I molecules themselves reside in or travel through the cellular compartments involved in MHC class II Ag processing and presentation.[65] Hence, the fusion of Ags with MHC class I molecule trafficking signals would redirect Ags into these compartments and allow the generation of MHC class II epitopes.[62] Correspondingly, immunization with optimized constructs carrying fused Ova as transgene AAV6/663-optOva (663-optOva) generated a more robust Ova-specific CD4$^+$ T cell response compared to AAV6/663-Ova (663-Ova), measured as IFNγ production in splenocytes stimulated with MHC class II Ova-specific peptide $Ova_{323–339}$ (Figure 2A). Increase in Ova-specific CD4$^+$ T cells coincided with a dramatic increase in levels of Ova-tetramer$^+$ CD8$^+$ T cells (Figure 2B). We next analyzed how vaccine optimization affects the Ova-tetramer$^+$ cell phenotype. Different populations of Ova-tetramer$^+$ cells were determined based on cell-surface markers as follows: effector cells as CD44$^+$/CD62L$^-$, terminally differentiated as CD44$^+$/CD62L$^-$/KLRG1$^+$/CD127$^-$, and effector memory precursor cells were determined as CD44$^+$/CD62L$^-$/KLRG1$^-$/CD127$^+$.[66] All Ova-tetramer$^+$ cells generated with either vaccine were CD44$^+$/CD62L$^-$ (Figure 2C). The percentages of KLRG1$^+$ terminally differentiated effector cells were comparable for both vaccines. However, 663-optOva led to significantly higher levels of KLRG1$^-$/CD127$^+$ precursor memory cells, which have the potential to become memory cells and are the positive indicators of vaccine quality (Figure 2D). We analyzed the functional activity of generated Ova-specific T cells 4 and 9 weeks post-immunization by IFNγ production in splenocytes and by *in vivo* killing of adoptively transferred syngeneic splenocytes pulsed with $Ova_{257–264}$ peptide (Figure 3). Mice immunized with 663-optOva released higher levels of IFNγ and displayed higher levels of killing capacity compared to immunization with 663-Ova (Figure 3). Importantly, the difference in efficacy was more significant after 9 weeks post-vaccination as in 663-optOva-vaccinated mice; 43.4% ± 11.8% of peptide-pulsed splenocytes were killed, compared to 5.2% ± 1.2% in 663-Ova-vaccinated mice (Figures 3D and 3E). These data show that Ag fusion with trafficking signals from the

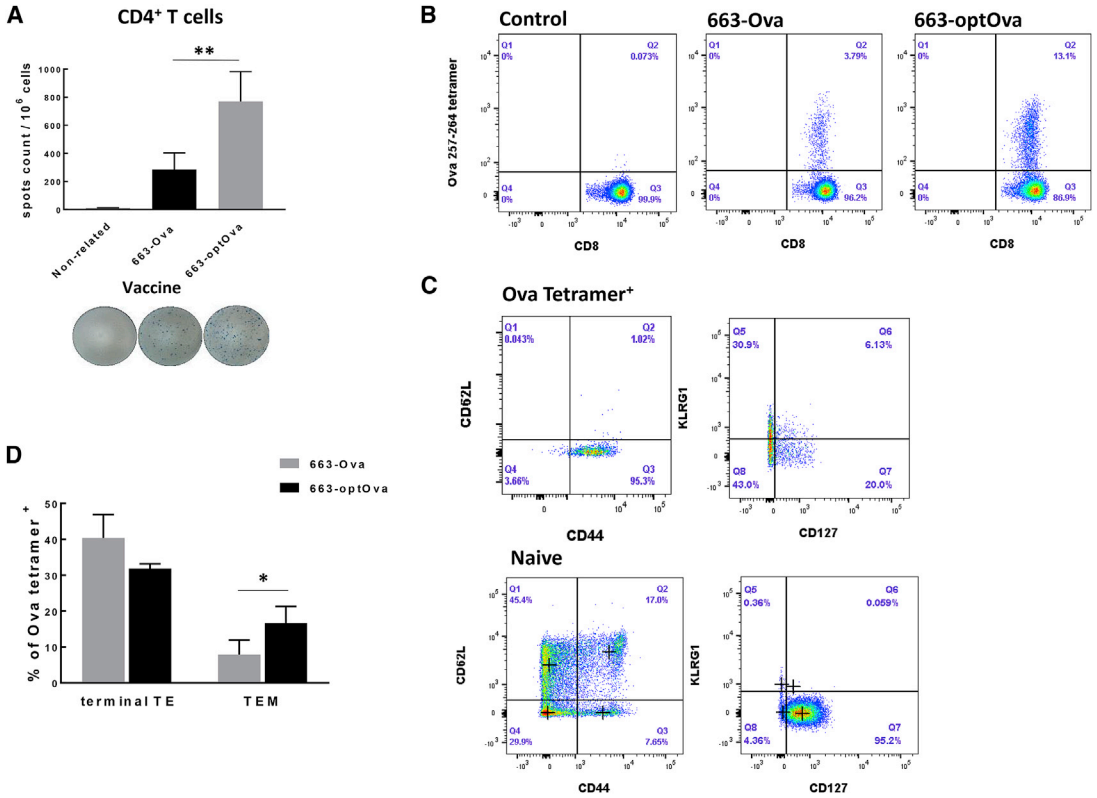

Figure 2. 663-optOva Has Superior Capacity to Generate an Ag-Specific Immune Response

(A) Analysis of IFNγ secretion by spleen $CD4^+$ T cells stimulated with MHC class II Ova-immunodominant peptide $Ova_{323–339}$ 2 weeks after immunization measured by ELISPOT assay. (B) Levels of $Ova_{257–264}$- tet^+ $CD8^+$ T cells in the blood 2 weeks after vaccination. (C) The representative analysis of changes in activation markers on cell surface of $Ova_{257–264}$- tet^+ $CD8^+$ T cells compared to naive cells in the blood 3 weeks after vaccination. OD, optical density. (D) Levels of terminally activated and memory precursor effector T cells after vaccination, which were calculated after analysis of data. Cell populations were defined as follows: T effector (TE) cells: $Ova_{257–264}$- $tet^+/CD44^+/CD62L^-$; terminally differentiated T effector (terminal TE): $Ova_{257–264}$- $tet^+/CD44^+/CD62L^-/KLRG1^+/CD127^-$; T effector memory (TEM): $Ova_{257–264}$- $tet^+/CD44^+/CD62L^-/KLRG1^-/CD127^+$; and T central memory (TCM): $Ova_{257–264}$-$tet^+/CD44^+/CD62L^+/KLRG1^-/CD127^+$. * $p < 0.05$.

MHC class I molecule significantly increases the potency of the AAV6-based vaccine by targeting both $CD4^+$ and $CD8^+$ T cells and by creating a higher number of memory cells.

Induction of Anti-tumor Protection after Vaccination

The vaccine's anti-cancer potential was tested against a highly aggressive syngeneic B16F10 melanoma tumor stably expressing Ova (B16/Ova). First, the vaccine's ability to prevent the spread of metastasis was investigated in a metastatic model after intravenous (i.v.) injection of tumor cells. Vaccination with intramuscular injections of 663-optOva demonstrated excellent protection against lung metastasis compared with non-relevant control. Vaccinated mice developed very few or no tumor nodules on lungs compared to non-vaccinated mice, which had more than 200 nodules 19 days after the injection of 5×10^5 tumor cells (Figure 4A). Second, in prophylactic solid tumor models, mice were immunized by intramuscular injection with 663-Ova or 663-optOva and then challenged with 5×10^5 B16/Ova cells inoculated intradermally into the right flank to mimic melanoma development. In this model, tumors formed in a distal site that was less exposed to circulating immune cells. Vaccination induced a significant delay in tumor growth (Figure 4B); on average, the tumor become noticeable 7 days later for 663-Ova and 10 days later for 663-optOva compared to non-immunized mice, although tumors eventually recapitulate in all mice (Figure 4C). To understand why the vaccination was only partially effective, we tested how well tumor cells retain Ova expression under the treatment. We analyzed tumor lysates by western blotting for Ova expression at day 25 after inoculation (Figure 4D). At this time point, B16/Ova cells continued to express Ova in tumors of non-immunized mice; however, in immunized mice, tumors completely lost the expression of Ova. Hence, the limited success of our vaccination in a solid tumor model can be explained in part by the loss of Ag expression, allowing tumors to escape elimination by vaccine-induced CTLs.

Vaccination Changes the Composition and Number of Immune Cells in Tumor

To understand how vaccination affects the immune landscape of tumors, the composition of immune cells in the tumor was

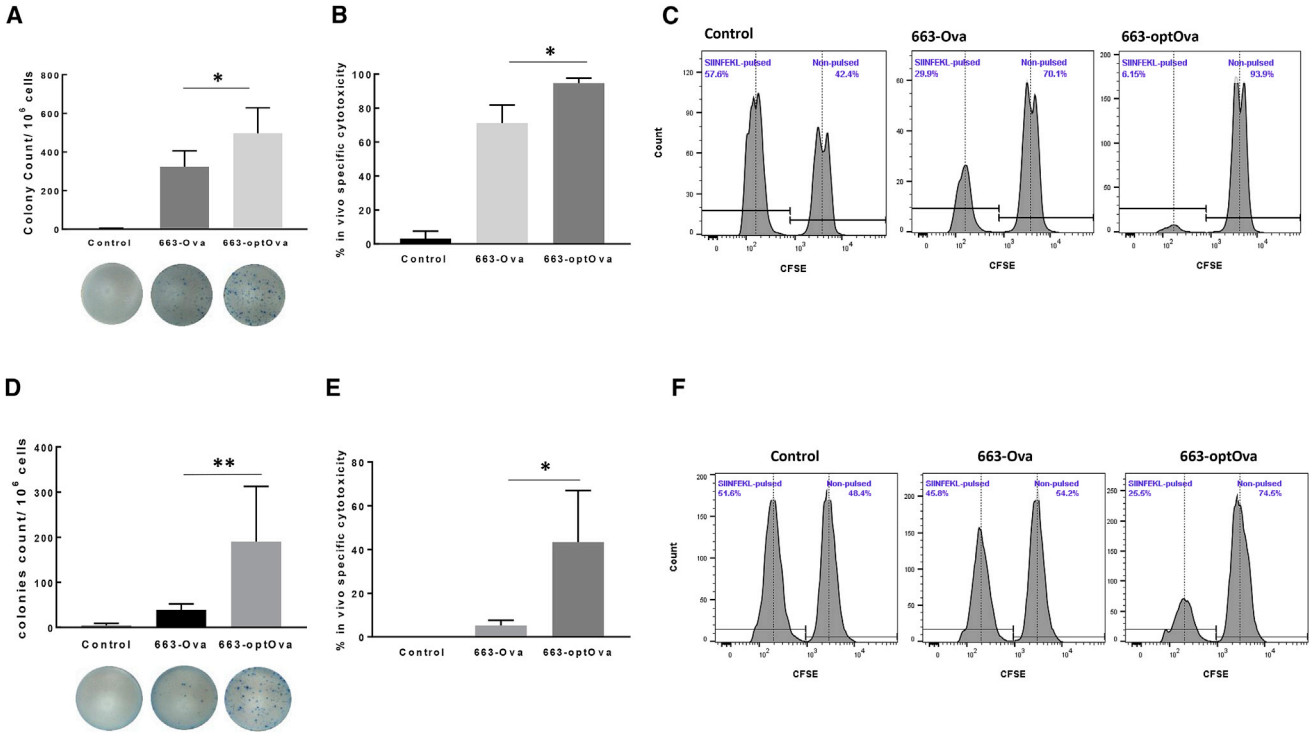

Figure 3. Comparison of Functional Activity of Ova-Specific CD8⁺ T Cells after 663-Ova and 663-optOva Vaccination

(A–C) Functional analysis 4 weeks after vaccination. (A) IFNγ production by splenocytes re-stimulated with $Ova_{257–264}$ peptide (SIINFEKL) 4 weeks after immunization. (B) *In vivo* cytotoxicity assay 4 weeks after immunization. Syngeneic naive splenocytes were divided into two equal parts and labeled with low and high concentrations of CFSE. The fraction labeled with low CFSE concentration was also pulsed with $Ova_{257–264}$ peptide before splenocytes were mixed and adoptively transferred to immunized mice. 16 h later, CFSE-labeled populations were analyzed in the spleen. (C) Representative results for each group. (D–F) Functional analysis 9 weeks after vaccination. (D) IFNγ production by splenocytes re-stimulated with $Ova_{257–264}$ peptide (SIINFEKL) 9 weeks after immunization. (E and F) *In vivo* killing capacity of mice immunized 9 weeks before analysis. 16 h after adoptive transfer of labeled splenocytes. *$p < 0.05$; **$p < 0.01$.

analyzed at day 11 after tumor inoculation. Since tumors in immunized mice are relatively hard to detect at this time point, B16/Ova cells were implanted with Matrigel, which forms a jelly plug. Flow cytometry analysis showed that tumor in non-immunized mice had a very limited number of $CD45^+$ immune cells, which comprised 3% of all counted cells. Most of these immune cells were tumor-associated macrophages (TAMs) and myeloid-derived suppressor cells (MDSCs), while $CD8^+$ T cells were largely absent (0.08% of all counted cells). Immunization induced dramatic infiltration of immune cells into the tumor. In 663-Ova- and 663-optOva-immunized mice, $CD45^+$ cells comprised 12% and 22% of all counted cells, respectively (Figures 5A and 5B). While an increase was noticeable in all analyzed populations, natural killer (NK) and T cells became the major populations of immune cells in the tumor after immunization (Figure 5B). In 663-optOva immunized mice, $CD8^+$ T cells comprised 3% of all counted cells and 21% of $CD45^+$ immune cells. In all analyzed tumors, infiltrating $CD8^+$ T cells were $CD44^+$, which indicates that they were activated by encountering Ags presented by APCs (Figure 5C). In immunized mice, 28% of tumor-infiltrating $CD8^+$ T cells were Ova-tetramer$^+$. At the same time, levels of Ova-tetramer$^+$ cells in the blood were 4% (Figure 5C).

We also analyzed the levels of PD-1 expression on $CD8^+$ T cells in the tumor and in the blood (Figure 5D). Ova-tetramer$^+$ cells in the tumor had higher levels of PD-1 expression (MFI = 935) compared to their counterpart in the blood (MFI = 447) (Figure 5D). In addition, half of non-Ova-specific CD8+ T cells in the tumor also had an increased expression of PD-1 (Figure 5E). Increased PD-1 expression on CTLs should sensitize them to anti-PD-1 antibody (aPD-1) treatment. We tested this hypothesis by combining vaccination with aPD-1 treatment. Mice were immunized with 663-optOva; 2 weeks later, they were challenged with intradermal injection of 5×10^5 B16/Ova cells. Anti PD-1 antibodies were injected intra-peritoneally every 3 days for five times in total. As expected, the combination of AAV vaccination and aPD-1 treatment significantly delayed tumor development up to 20 days (Figures 5F and 5G).

In summary, we concluded that the vaccine successfully generates antigen-specific CTLs, which infiltrate the tumor. Moreover, the vaccine

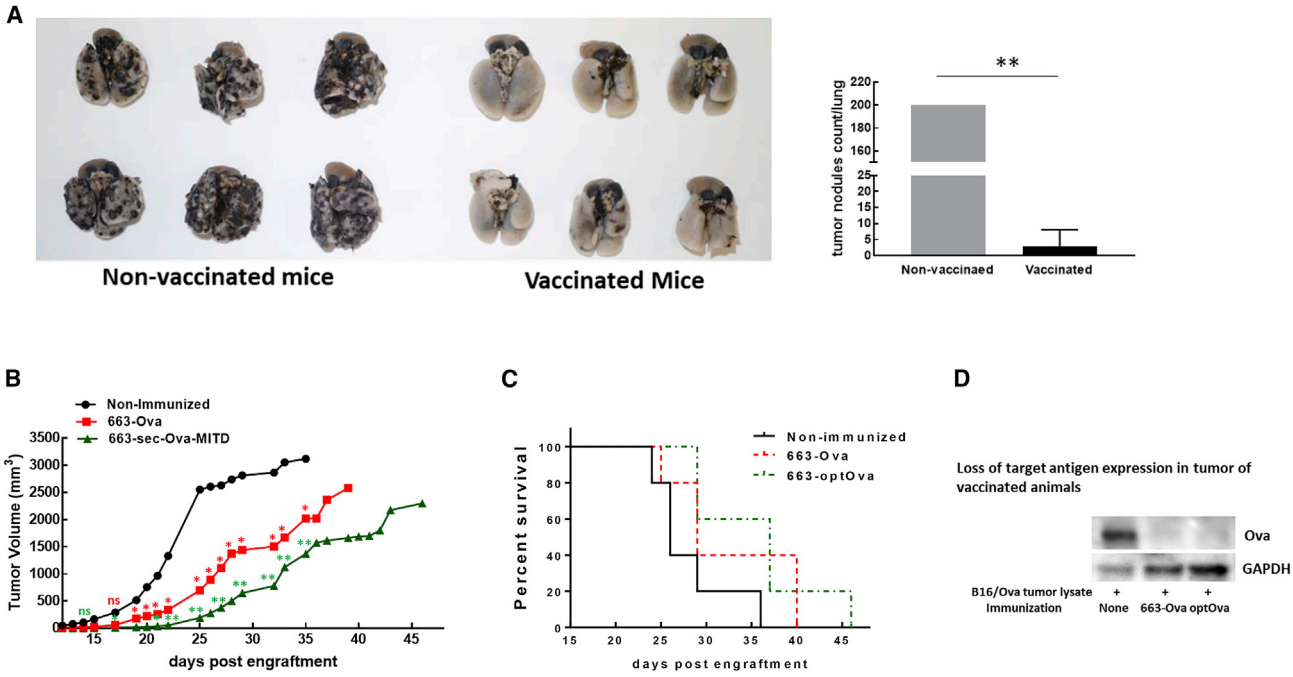

Figure 4. Analysis of Vaccine Effectiveness against B16/Ova Tumor

(A) Prophylactic 663-optOva vaccination gives protection against metastatic tumor spread. B16/Ova metastatic nodules are visible as black dots. Vaccinated mice had 0–13 B16/Ova nodules on the lungs. Non-vaccinated mice all had more than 200 B16/Ova nodules on lungs, so all values were marked as 200 for the purpose of this graph (right panel). Left panel: images of lungs. **$p < 0.01$. (B) Growth of intradermal B16/Ova tumor implanted on mouse flanks 2 weeks after vaccination. Statistical differences between groups were assessed by one-way ANOVA, vaccinated versus non-immunized. *$p < 0.05$; **$p < 0.01$; ns, non-significant. (C) Kaplan-Meyer survival plots of animals depicted in (B). (D) Post-necroptic analysis of Ova expression in tumor by western blotting on day 25 after tumor implantation.

facilitates the infiltration of tumor with other immune cells in addition to Ova-specific T cells.

AAV6-Based Vaccine Can Break the Tolerance to Tumor-Associated Antigens that Are Non-mutated Self-Proteins

While Ova is an ideal antigen to assess the immune reactions, we wanted to test whether the vaccine we designed can successfully generate CTLs against tumor-associated antigens (TAAs), which are frequently endogenous non-mutated proteins. For melanoma, several TAAs are well described,[33] so we developed a vaccine against two melanosomal differentiation antigens: Tyr and gp100. Both vaccines encode xenogeneic (human) sequences, which have been shown to be able to facilitate immune recognition of self-proteins.[67,68] Mice were immunized with 10^{10} vector genome of either vaccine by intramuscular injection; two weeks later, mice were sacrificed, and the ability of splenocytes to produce IFNγ and TNF-α was analyzed by ELISPOT assay. After both vaccines, 663-optTyr and 663-opt-gp100 splenocytes responded to re-stimulation by producing IFNγ and TNF-α, indicating that the vaccines were able to break the tolerance (Figures 6A and 6B).

DISCUSSION

Several studies highlighted the usefulness of certain AAV serotypes for immunomodulation and cancer vaccines, depending on capsid configuration, dose, and route of administration in a mouse model.[14–19] Among other serotypes, AAV6 is able to transduce the cells of myeloid origin in general[39,69] and DCs in particular.[25,35] Thus, AAV6-based vectors with Ova as a model Ag as described here are a highly attractive platform for developing anti-tumor vaccines. The ability of AAV6 to stimulate Ag-specific immune responses was shown before, though the direct DC targeting *in vivo* after intramuscular injection has not been shown. We were able to track down DCs expressing the reporter gene GFP in draining lymph nodes 4 days after intramuscular injection of scAAV6-663-CMV-GFP by flow cytometry and microscopic analysis (Figures 1D and 1E). These experiments are not ruling out the importance of cross-presentation from DCs picking up material from dying muscle cells infected with AAV-GFP, particularly since AAV6 vectors infect muscle cells with high efficiency.[70] However, the high levels of GFP fluorescence that we observed in DCs from drained lymph nodes are most likely induced by direct AAV-mediated expression of GFP in DCs. Our data are in line with the earlier published observation that AAV6 DNA can be detected in lymph nodes after oral administration.[18] Next, we showed that a single intramuscular injection of sc 663-Ova driven by a CMV promoter induced strong Ova-specific $CD8^+$ T cell and humoral responses. The generation of Ag-specific cytotoxic $CD8^+$ T cells is an ultimate goal of an efficient cancer vaccine. However, the quality and killing capability of generated $CD8^+$ T cells

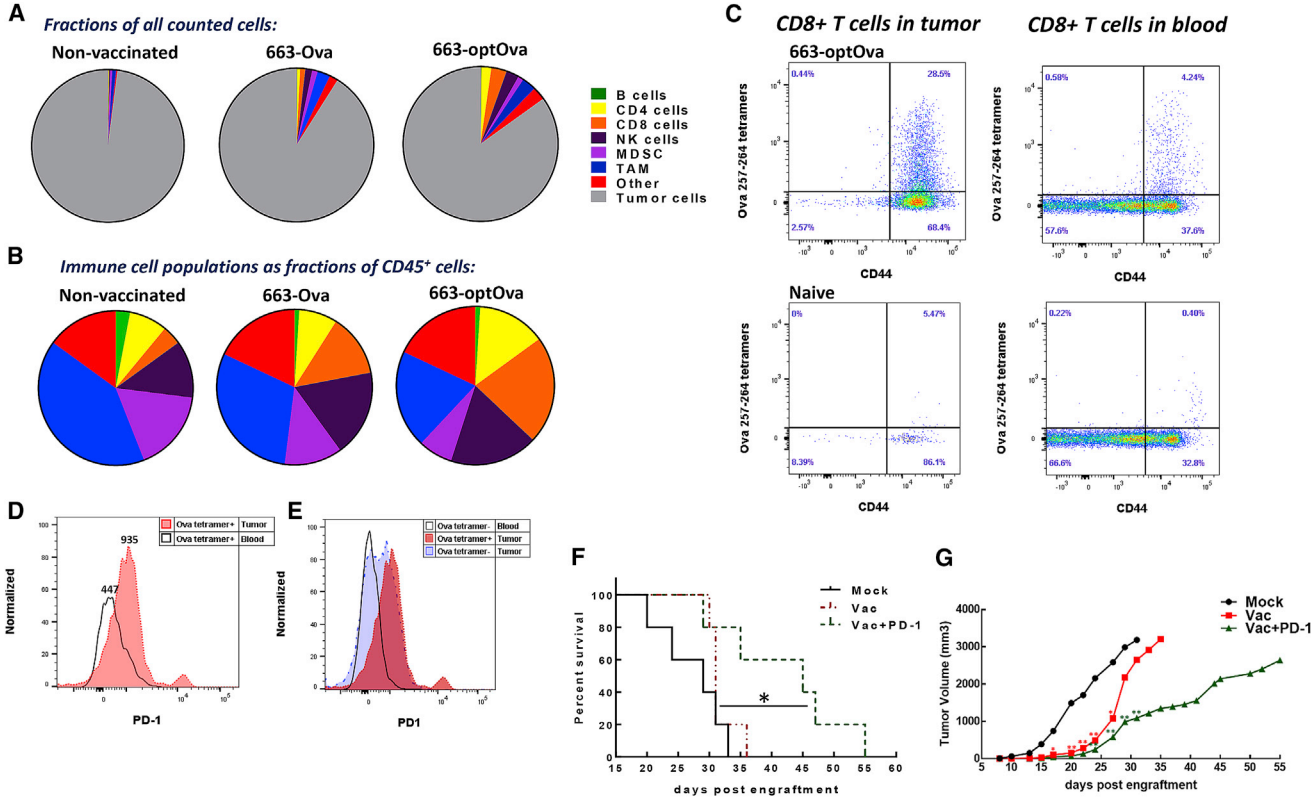

Figure 5. Analysis of Immune Cell Populations in the Blood and Tumor of Tumor-Bearing Mice

(A) Fraction of each cell population relative to all cells counted in the tumor. (B) Immune cell populations as a fraction of $CD45^+$ cells. For (A) and (B), immune cell populations were determined as follows: total immune cells, $CD45^+$; B cells, $CD45^+/CD3^-/CD19^+$; T cells, $CD45^+/CD19^-/CD3^+$; $CD4^+$ T cells, $CD45^+/CD19^-/CD3^+/CD8^-/CD4^+$; $CD8^+$ T cells, $CD45^+/CD19^-/CD3^+/CD4^-/CD8^+$; NK cells, $CD45^+/CD19^-/CD3^-/NK1.1^+$; TAMs, $CD45^+/CD3^-/CD11b^+/F4/80^+$; and MDSCs, $CD45^+/CD11b^+/Gr\text{-}1^+$. (C) $Ova_{257–264}$-tet^+ CD8+ T cells in blood and tumor. (D) $Ova_{257–264}$-tet^+ CD8+ T cells have higher PD-1 expression in tumors compared to $Ova_{257–264}$-tet^+ CD8+ T cells in blood. (E) PD-1 expression on Ova- and non-Ova-specific $CD8^+$ T cells in tumors of 663-optOva-vaccinated mice compared to non-related $CD8^+$ T cells in the blood. (F and G) Effect of adding aPD-1 treatment to the vaccination on tumor growth and survival. Mice were vaccinated with 663-optOva, and 2 weeks later, B16/Ova was implanted intradermally. aPD-1 treatment started by injection of 200 μg PD-1 antibodies i.p. twice a week starting on day 3 after tumor injection, for a total 5 doses. (F) Kaplan-Meier survival curves. *$p < 0.05$, log-rank Mantel-Cox test. (G) Growth of tumor. Statistical differences between groups were assessed by one-way ANOVA, vaccinated versus non-immunized. *$p < 0.05$; **$p < 0.01$; ns, non-significant.

depend on cognate $CD4^+$ T cell help. To enhance the generation of Ag-specific $CD4^+$ T cells, we fused Ags with trafficking signals of MHC class I molecules to facilitate processing through the endosome/lysosome pathway and presentation on MHC class II molecules.[62] We confirmed that these modifications of Ag results in higher levels of both $CD4^+$ and $CD8^+$ Ag-specific T cells. Generated Ova-specific $CD8^+$ T cells had improved effector functions, including increased IFNγ production and killing capacity (Figure 3). The optimized vaccine also elicited more effector memory precursor ($CD62L^-/CD127^+$) cells, which ensured a long-lasting anti-tumor immune response. Consequently, we confirmed Ova-specific T cells to be highly active 2 months after vaccination. All optimizations described earlier allowed us to use our AAV vaccine at relatively low doses: through these experiments, we used 10^{10} vg per mouse (less than 5×10^{11} vg/kg), though doses as low as 2.5×10^9 vg per mouse generated sufficient cytotoxic responses (data not shown). Gene therapy clinical trials with AAV typically use higher doses, in the range of 10^{13} vg/kg, which are well tolerated.[13] Moreover, we used doses that are lower than doses published for other serotypes of AAV suitable for vaccine development. AAVrh32.33 was used at doses of 3×10^{10} to 1×10^{11} vgs per mouse,[24,71,72] and AAV1 was used at a dose of 2×10^{11} vgs per mouse.[19]

The vaccine we designed was tested in B16/Ova melanoma tumor models. It protected well in prophylactic vaccination against metastatic tumor spread when B16/Ova cells were administered in i.v. injections. When B16/Ova cells were transplanted intradermally and formed solid tumors, vaccination delayed tumor growth and overall survival but did not completely prevent its occurrence. The vaccine's inability to eradicate solid tumors could be partially explained by the tumor's loss of Ag expression, as it is a well-documented form of escape from the anti-tumor immune system attack.[73–75] Thus, in our future studies, we plan to increase the number of targets recognized by the vaccine to reduce the potential of the tumor to escape treatment.

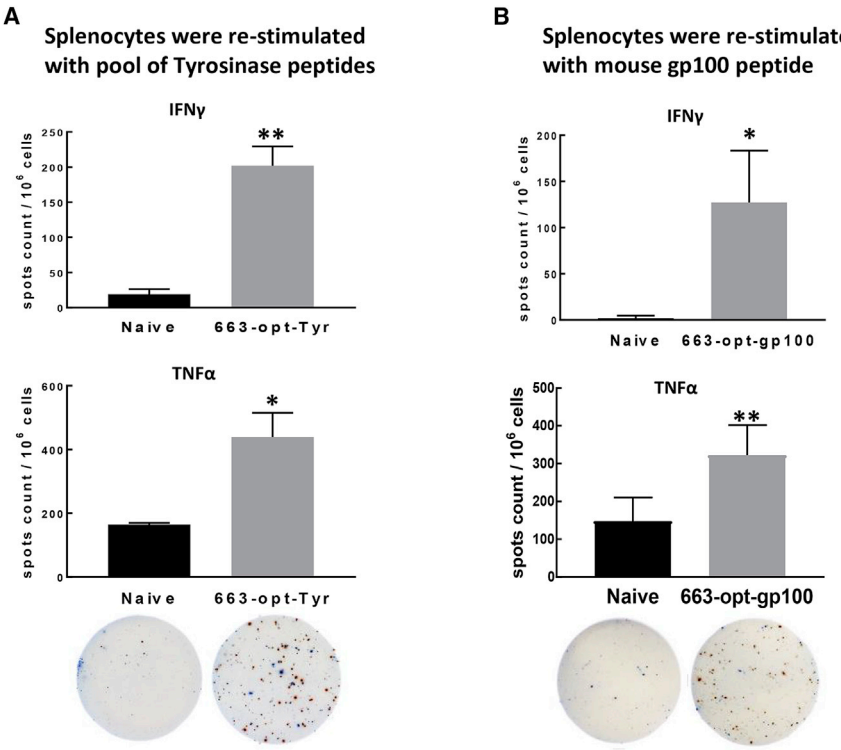

Figure 6. Breaking Tolerance to TAAs Derived from Non-mutated "Self-Proteins"

(A and B) Mice were immunized with 663-optTyr (A) or 663-opt-gp100 (B) vaccine. (A) Two weeks later, the antigen-specific T cell response against tyrosinase was determined in splenocytes re-stimulated with overlapping tyrosinase peptide mixture (PepMix) by IFNγ and TNF-α ELISPOT assay. (B) Splenocytes from mice immunized with 663-opt-gp100 were stimulated with H-2Db-restricted epitope mouse $GP100_{25–33}$ EGSRNQDWL. On representative ELISPOT images, red spots indicate IFNγ, and blue spots indicate TNF-α. *$p < 0.05$; **$p < 0.01$.

Considering the complexity of tumor immunity, it is not expected that a therapeutic vaccine should act as a monotherapy.[6] The immunosuppressive nature of TME is another possible reason why the AAV-vaccine-generated CTLs are not able to eradicate a tumor.[76] The TME is characterized by multiple immunosuppressive mechanisms that dampen anti-tumor CTL activity, including T cell anergy, extrinsic suppression by regulatory T cells and immunosuppressive cell populations, inhibition by ligation of negative regulatory receptors, and metabolic perturbations.[76] The combination of a vaccination with the therapy that maintains CTLs in an active state inside the tumor and/or ameliorates the immunosuppressive TME should significantly improve anticancer treatment. Good candidates for combinatorial treatments are antibodies targeting PD-1-PD-L1 interaction.[77,78] B16 melanoma is one of the therapy-resistant tumors including the absence of response to aPD-1 monotherapy.[79,80] The B16 tumor immune profile showed that, without any treatment, it was infiltrated by a small number of $CD8^+$ T cells. The immune cells were represented mainly by immunosuppressive MDSCs and TAMs and composed 3% of the tumor (Figure 5). Therefore, one of the reasons why the B16 tumor does not respond to single aPD-1 therapy is the absence of infiltrated CTLs, which can be reactivated by aPD-1 therapy. Consequently, one of our important findings is that AAV vaccination resulted in massive immune cell infiltration of tumor. 28% of CTLs inside the tumor were Ag specific and exhibited higher levels of PD-1 expression compared to the same cell's type found in the blood. Additionally, the tumor was also inflamed with non-Ova-specific CTLs and NK cells. We hypothesized that the increased number of tumor-infiltrated lymphocytes and enhanced expression of PD-1 should overturn resistance of the B16 tumor to aPD-1 therapy. Indeed, AAV-based vaccination in combination with aPD-1 treatment significantly delayed tumor development and extended mouse survival (Figure 5).

The experiments with Ova as an Ag prove that an AAV6-based vaccine is a good platform for anticancer vaccine design. However, Ova is an artificially introduced antigen, while tumor-associated antigens are generally non-mutated self-proteins. It was important to show that the vaccine can break immune tolerance toward self-antigens. To test vaccine against endogenous antigens, we used Tyr and gp100. Immunization with AAV6-based vaccines induced CTLs against both self-proteins. These data ensure that the AAV6-based vaccine is a powerful tool and can be designed for clinically relevant targets.

In summary, we designed an AAV-based vaccine with superior cytolytic capacity against an encoded antigen. This vaccine prevents metastatic tumor spread, significantly delays solid tumor growth, and synergizes with emerging aPD-1 therapy. More importantly, the vaccination changes the immune landscape of the tumor by inducing tremendous infiltration of the tumor with immune cells, especially with CD8+ T cells and NK cells. Therefore, what we are planning to implement to completely eradicate tumors is vaccination in concert with other therapies that target the tumor microenvironment and re-activate/support immune cells infiltrating the tumor.

MATERIALS AND METHODS

Mice

Six- to 10-week-old male C57BL/6 mice were obtained from Jackson Laboratories (Bar Harbor, ME, USA). All manipulations with the animals were performed according to the principles of the National Research Council's Guide for the Care and Use of Laboratory Animals, with approval from the University of Minnesota Institutional Animal Care and Use Committee (IACUC).

AVV6-Based Vaccine Construct Design and Production

The sc expression cassettes with Ova or GFP, human tyrosinase (TYR), and human premelanosome protein (gp100) driven by

Table 1. Nomenclature of AAV Constructs

AAV Vector Construct Abbreviation Used in This Article	Full Name of AAV Vector Construct	Brief Description
WT-AAV6	wild type-AAV6	unmodified capsid
663-AAV6	AAV6-S663V	capsid optimization with substitution of serine at position 663 to valine
663-Ova	AAV6-S663V-CMV-Ova	modified AAV vector expressing unmodified ovalbumin
663-GFP	AAV6-S663V-CMV-GFP	modified AAV vector expressing GFP
optOva	CMV-Sec-Ova-MITD	expression cassette with ovalbumin fused with MHC class I leader (Sec) and trafficking signal (MITD) peptides
663-optOva	AAV6-S663V-CMV-Sec-Ova-MITD	modified AAV vector expressing modified ovalbumin
663-optTyr	AAV6-S663V-CMV-Sec-Tyrosinase-MITD	modified AAV vector expressing modified tyrosinase
663-opt-gp100	AAV6-S663V-CMV-Sec-gp100-MITD	modified AAV vector expressing modified gp100

CMV promoters were packaged in AAV serotype 6 (AAV 2/6) WT or containing a single mutation on the VP3 capsid protein at amino acid (aa) 663 to substitute serine (S) for valine (V).[21] Fusion of the transgene with the N-terminal leader peptide (Sec) and MHC class I trafficking signal (MITD) attached to the C-terminus was performed as described previously.[62] As a source of MHC class I signal peptide (Sec, 78 bp), and MHC class I trafficking signal including the stop codon (MITD, 168 bp), we used the sequence of human MHC class I gene HLA-B*15 (NCBI: NM_005514.8). A summary of abbreviations and nomenclature of vectors used in this study is presented in Table 1. Vectors were packaged in HEK293 cells and isolated by iodixanol gradient followed by ion-exchange column purification as described previously.[21]

In Vivo *Cytotoxicity Measurement*

The cytotoxic efficacy of Ova-reactive CD8 T cells was determined *in vivo* as described previously.[81,82] Briefly, naive splenocytes from C57BL/6 were isolated, and divided into two equal parts, and stained with 5 or 0.4 μM carboxyfluorescein succinimidyl ester (CFSE). The latter fraction was pulsed with 10 μM of Ova 257–264 peptide (SIINFEKL) and then combined with the first (non-pulsed) fraction. The mixture of 5×10^6 to 10×10^6 cells was administered in an i.v. injection into recipient mice. After 4–16 h, the splenocytes of recipient mice were analyzed by flow cytometry, and the percentage of specific lysis was calculated from the reduction of peptide-pulsed $CFSE^{dim}$ target cells relative to non-pulsed $CFSE^{hi}$ reference cells.

Enzyme-Linked Immunospot Assay

For analysis of Ova-specific T cells, IFNγ response to re-stimulation of splenocytes with Ova-immunodominant peptides (AnaSpec) MHC class I $Ova_{257–264}$ and MHC class II $Ova_{323–339}$ was measured by standard ELISPOT assay (Cellular Technology, Shaker Heights, OH, USA) according to the manufacturer's protocol. For analysis of Tyr- and gp100-specific T cells, IFNγ and TNF-α were measured in re-stimulated splenocytes by the double-color mouse IFNγ/TNFα ImmnunoSpot system (Cellular Technology, Shaker Heights, OH, USA). Splenocytes from the mice immunized with 663-optTyr were re-stimulated with the pool of human Tyr peptides (JPT Peptide Technologies). Splenocytes from 663-opt-gp100-immunized mice were re-stimulated with mouse gp100 peptide epitope $mGP100_{25–33}$ EGSRNQDWL (AnaSpec). For all experiments, splenocytes were seeded at 5×10^5 cells per well and were stimulated with corresponding peptides at a final concentration of 5 μg/mL. Plates were cultured for 24 h and then developed according to the manufacturer's instructions. The IFNγ- and TNF-α-secreting spots were counted with an ELISPOT reader. Results are presented as number of spots per 10^6 cells.

Ovalbumin Antibody Detection

ELISA plates (Immulon, Thermo Fisher Scientific) were coated overnight with 10 μg/mL purified Ova (Millipore) diluted in Voeller's buffer. The next day, wells were blocked with 1% BSA in PBS for 1 h at room temperature. Mouse sera were diluted from 1:50 to 1:3,200 with 1% BSA in PBS and added to wells for 2 h. Goat anti-mouse immunoglobulin G-horseradish peroxidase (IgG-HRP) conjugate (Bio-Rad) was used as a secondary antibody at a dilution of 1:3,000. Plates were developed with Turbo TMB substrate (Thermo Fisher Scientific), and the colorimetric reaction was stopped with 2 M H_2SO_4. Plates were read at 450 nm with a BioTek Instruments microplate reader.

Western Blotting

B16/Ova tumor was homogenized in RIPA lysis buffer supplemented with anti-protease inhibitors. Lysates were clarified by centrifugation, protein concentration was measured with the Pierce BCA Protein Assay Kit (Thermo Fisher Scientific), and equal amounts of protein were loaded on 10% SDS-PAGE gels. Ova expression was detected with rabbit polyclonal Ova antibodies (Millipore), and GAPDH expression was used as endogenous control. Imaging was performed on ah AI600 imager (Amersham).

Tumor Challenge Experiments

B16/Ova was created by transfection of B16F10 cells with pCDNA3-Ova plasmid (Addgene) and subsequent selection of clones on media with 500 μg/mL G418. The stability of Ova expression in selected clones was confirmed by culturing clones in media without selective antibiotic and monitoring Ova expression by western blotting or ELISA for at least for 1 month.

In the prophylactic tumor challenge study, mice were vaccinated with a single intramuscular injection of 10^{10} vg 663-optOva, 663-Ova, or

PBS (in some experiments, 663-Luciferase was used as a non-related vaccine for control). 14 days post-vaccination, mice were injected in the flank intradermally with 5×10^5 B16/Ova cells. Indicated mice were treated with anti-PD-1 antibodies (RMP-114, Bioxcell) (200 μg per mouse, intraperitoneally (i.p.) twice a week starting on day 3 after tumor injection, for a total 5 doses). A digital caliper was used to measure tumors every other day, and the products of the perpendicular diameters were recorded. Mice were euthanized when tumor diameter exceeded 20 mm or when severe lesional ulcerations developed. For analysis of the immune cells infiltrating tumors, B16/Ova cells were resuspended in Matrigel before injections as described by Fridman et al.[83] 11 days after tumor inoculation, Matrigel plaques were excised, and pieces of equal weight were processed and standardized with counting beads for flow cytometry assays.

In the metastatic model, mice were immunized by a single intramuscular injection of 10^{10} vg of 663-optOva (6 mice in each group). 2 weeks post-vaccination, mice were injected with 5×10^5 B16/Ova cells in the tail vein. 19 days after tumor challenge, mice were euthanized, and lungs were briefly rinsed with tap water to remove blood and were bleached overnight in Fekete's solution. The next day, B16 tumor nodules, visible as black dots, were counted on lungs.[33]

Isolation of Immune Cells from Blood, Spleens, Lymph Nodes, and Tumors

Blood was collected by cheek bleeding, erythrocytes were removed by adding red blood cells (RBC) lysis buffer, and cells were washed twice with PBS and resuspended in flow staining buffer (1% fetal bovine serum [FBS] in PBS plus 0.025% sodium azide). Spleens were homogenized by passing through a cell strainer, gently applying the syringe plunger; and erythrocytes were removed by applying RBC lysis buffer. Spleen single-cell suspensions were kept in RPMI medium (#A10491, ATCC modification, GIBCO) supplemented with 10% heat-inactivated FBS (GIBCO), 100 U/mL penicillin, 100 μg/mL streptomycin, for functional assays, or in flow staining buffer for analysis by flow cytometry.

Drained lymph nodes and tumors were harvested, cut into small pieces, and incubated with 100 μg/mL collagenase D and 10 μg/mL DNase I (Roche) for 30 min at 37°C with frequent mixing. At the end of the incubation, tissues were pushed through a cell strainer using a syringe plunger to obtain cell suspensions, and erythrocytes were removed by adding RBC lysis buffer. Cells were washed twice with PBS and re-suspended in flow staining buffer.

Flow Cytometry and Antibodies

The following fluorophore-conjugated antibodies to mouse were purchased from BioLegend: CD45 (30-F11), CD3e (145-2C11), CD4 (RM4-5), CD11c (N418), CD11b (M1/70), Gr-1 (RB6-8C5), CD44 (IM7), MHC II (I-A/I-E) (M5/114.15.2), F4/80 (BM8), NK1.1 (PK136), CD127 (A7R34), and CD19 (6D5). CD62L (MEL-14), PD-1 (J43), and KLRG1 (2F1) were obtained from BD Biosciences. CD8 (KT15) was from Thermo Fisher Scientific, and ova-specific H-2K^b MHC class I tetramers (Ova 257-264 tetramers) were purchased from MBL International. Before staining with cell-surface markers, FcRs were blocked with CD16/CD32 (2.4G2, BD Biosciences) antibodies. Dead cells were excluded by positive staining with 7-AAD (BioLegend). Cells were analyzed using the BD FACS LSRFortessa or BD FACSAria II, and data were analyzed with FlowJo.

Statistical Analysis

All data are shown as mean ± SEM. For all statistical analyses, an unpaired t test was used. Data were considered significant when p values were <0.05.

AUTHOR CONTRIBUTIONS

K.K. and G.A. developed the concept of the project and designed experiments. K.K. and A.D. performed experiments. K.K. and G.A. wrote the manuscript. A.D. reviewed and edited the manuscript.

CONFLICTS OF INTEREST

Karina Krotova and Andrew Day declare no competing interests. George Aslanidi holds issued patents related to AAV vectors that have been licensed to various gene therapy companies.

ACKNOWLEDGMENTS

This project is supported by startup funds from the Hormel Institute. The authors thank Josh Moth for editing the manuscript.

REFERENCES

1. Rosenberg, S.A., Yang, J.C., and Restifo, N.P. (2004). Cancer immunotherapy: moving beyond current vaccines. Nat. Med. *10*, 909–915.
2. Rosenberg, S.A., and Restifo, N.P. (2015). Adoptive cell transfer as personalized immunotherapy for human cancer. Science *348*, 62–68.
3. McGray, A.J.R., Hallett, R., Bernard, D., Swift, S.L., Zhu, Z., Teoderascu, F., Vanseggelen, H., Hassell, J.A., Hurwitz, A.A., Wan, Y., and Bramson, J.L. (2014). Immunotherapy-induced CD8+ T cells instigate immune suppression in the tumor. Mol. Ther. *22*, 206–218.
4. Martin Lluesma, S., Wolfer, A., Harari, A., and Kandalaft, L.E. (2016). Cancer vaccines in ovarian cancer: how can we improve? Biomedicines *4*, 10.
5. Hollingsworth, R.E., and Jansen, K. (2019). Turning the corner on therapeutic cancer vaccines. NPJ Vaccines *4*, 7.
6. Melief, C.J.M., van Hall, T., Arens, R., Ossendorp, F., and van der Burg, S.H. (2015). Therapeutic cancer vaccines. J. Clin. Invest. *125*, 3401–3412.
7. Mendell, J.R. (2018). Therapy for spinal muscular atrophy. N. Engl. J. Med. *378*, 487.
8. Mingozzi, F., and High, K.A. (2011). Therapeutic in vivo gene transfer for genetic disease using AAV: progress and challenges. Nat. Rev. Genet. *12*, 341–355.
9. Mueller, C., and Flotte, T.R. (2008). Clinical gene therapy using recombinant adeno-associated virus vectors. Gene Ther. *15*, 858–863.
10. Corti, M., Liberati, C., Smith, B.K., Lawson, L.A., Tuna, I.S., Conlon, T.J., Coleman, K.E., Islam, S., Herzog, R.W., Fuller, D.D., et al. (2017). Safety of intradiaphragmatic delivery of adeno-associated virus-mediated alpha-glucosidase (rAAV1-CMV-hGAA) gene therapy in children affected by Pompe disease. Hum. Gene Ther. Clin. Dev. *28*, 208–218.
11. Feuer, W.J., Schiffman, J.C., Davis, J.L., Porciatti, V., Gonzalez, P., Koilkonda, R.D., Yuan, H., Lalwani, A., Lam, B.L., and Guy, J. (2016). Gene therapy for Leber hereditary optic neuropathy: initial results. Ophthalmology *123*, 558–570.
12. Keeler, A.M., and Flotte, T.R. (2019). Recombinant adeno-associated virus gene therapy in light of Luxturna (and Zolgensma and Glybera): where are we, and how did we get here? Annu. Rev. Virol. *6*, 601–621.

13. Gernoux, G., Wilson, J.M., and Mueller, C. (2017). Regulatory and exhausted T cell responses to AAV capsid. Hum. Gene Ther. *28*, 338–349.

14. Pulendran, B., and Ahmed, R. (2011). Immunological mechanisms of vaccination. Nat. Immunol. *12*, 509–517.

15. Xin, K.-Q., Mizukami, H., Urabe, M., Toda, Y., Shinoda, K., Yoshida, A., Oomura, K., Kojima, Y., Ichino, M., Klinman, D., et al. (2006). Induction of robust immune responses against human immunodeficiency virus is supported by the inherent tropism of adeno-associated virus type 5 for dendritic cells. J. Virol. *80*, 11899–11910.

16. Gross, D.-A., Ghenassia, A., Bartolo, L., Urbain, D., Benkhelifa-Ziyyat, S., Lorain, S., Davoust, J., and Chappert, P. (2019). Cross-presentation of skin-targeted recombinant adeno-associated virus 2/1 transgene induces potent resident memory $CD8^+$ T cell responses. J. Virol. *93*, e01334–e01318.

17. Carpentier, M., Lorain, S., Chappert, P., Lalfer, M., Hardet, R., Urbain, D., Peccate, C., Adriouch, S., Garcia, L., Davoust, J., and Gross, D.A. (2015). Intrinsic transgene immunogenicity gears CD8(+) T-cell priming after rAAV-mediated muscle gene transfer. Mol. Ther. *23*, 697–706.

18. Steel, J.C., Di Pasquale, G., Ramlogan, C.A., Patel, V., Chiorini, J.A., and Morris, J.C. (2013). Oral vaccination with adeno-associated virus vectors expressing the Neu oncogene inhibits the growth of murine breast cancer. Mol. Ther. *21*, 680–687.

19. Hensel, J.A., Khattar, V., Ashton, R., and Ponnazhagan, S. (2018). Recombinant AAV-CEA tumor vaccine in combination with an immune adjuvant breaks tolerance and provides protective immunity. Mol. Ther. Oncolytics *12*, 41–48.

20. Aslanidi, G.V., Rivers, A.E., Ortiz, L., Govindasamy, L., Ling, C., Jayandharan, G.R., Zolotukhin, S., Agbandje-McKenna, M., and Srivastava, A. (2012). High-efficiency transduction of human monocyte-derived dendritic cells by capsid-modified recombinant AAV2 vectors. Vaccine *30*, 3908–3917.

21. Pandya, J., Ortiz, L., Ling, C., Rivers, A.E., and Aslanidi, G. (2014). Rationally designed capsid and transgene cassette of AAV6 vectors for dendritic cell-based cancer immunotherapy. Immunol. Cell Biol. *92*, 116–123.

22. Rossi, A., Dupaty, L., Aillot, L., Zhang, L., Gallien, C., Hallek, M., Odenthal, M., Adriouch, S., Salvetti, A., and Büning, H. (2019). Vector uncoating limits adeno-associated viral vector-mediated transduction of human dendritic cells and vector immunogenicity. Sci. Rep. *9*, 3631.

23. Porgador, A., Irvine, K.R., Iwasaki, A., Barber, B.H., Restifo, N.P., and Germain, R.N. (1998). Predominant role for directly transfected dendritic cells in antigen presentation to CD8+ T cells after gene gun immunization. J. Exp. Med. *188*, 1075–1082.

24. Lin, J., Calcedo, R., Vandenberghe, L.H., Bell, P., Somanathan, S., and Wilson, J.M. (2009). A new genetic vaccine platform based on an adeno-associated virus isolated from a rhesus macaque. J. Virol. *83*, 12738–12750.

25. Pandya, M., Britt, K., Hoffman, B., Ling, C., and Aslanidi, G.V. (2015). Reprogramming immune response with capsid-optimized AAV6 vectors for immunotherapy of cancer. J. Immunother. *38*, 292–298.

26. Shedlock, D.J., Whitmire, J.K., Tan, J., MacDonald, A.S., Ahmed, R., and Shen, H. (2003). Role of CD4 T cell help and costimulation in CD8 T cell responses during *Listeria monocytogenes* infection. J. Immunol. *170*, 2053–2063.

27. Yao, Y., Li, P., Singh, P., Thiele, A.T., Wilkes, D.S., Renukaradhya, G.J., Brutkiewicz, R.R., Travers, J.B., Luker, G.D., Hong, S.C., et al. (2007). Vaccinia virus infection induces dendritic cell maturation but inhibits antigen presentation by MHC class II. Cell. Immunol. *246*, 92–102.

28. Matzinger, P. (2002). The danger model: a renewed sense of self. Science *296*, 301–305.

29. van den Boorn, J.G., Barchet, W., and Hartmann, G. (2012). Nucleic acid adjuvants: toward an educated vaccine. In Advances in Immunology, *Volume 114*, C.J.M. Melief, ed. Advances in Immunology (Academic Press), pp. 1–32.

30. Zaiss, A.-K., Liu, Q., Bowen, G.P., Wong, N.C.W., Bartlett, J.S., and Muruve, D.A. (2002). Differential activation of innate immune responses by adenovirus and adeno-associated virus vectors. J. Virol. *76*, 4580–4590.

31. Overwijk, W.W., Tsung, A., Irvine, K.R., Parkhurst, M.R., Goletz, T.J., Tsung, K., Carroll, M.W., Liu, C., Moss, B., Rosenberg, S.A., and Restifo, N.P. (1998). gp100/pmel 17 is a murine tumor rejection antigen: induction of "self"-reactive, tumoricidal T cells using high-affinity, altered peptide ligand. J. Exp. Med. *188*, 277–286.

32. Buitrago, E., Hardré, R., Haudecoeur, R., Jamet, H., Belle, C., Boumendjel, A., Bubacco, L., and Réglier, M. (2016). Are human tyrosinase and related proteins suitable targets for melanoma therapy? Curr. Top. Med. Chem. *16*, 3033–3047.

33. Overwijk, W.W., and Restifo, N.P. (2000). B16 as a mouse model for human melanoma. Curr. Protoc. Immunol. *39*, 20.21.21–20.21.29.

34. Aldrich, W.A., Ren, C., White, A.F., Zhou, S.Z., Kumar, S., Jenkins, C.B., Shaw, D.R., Strong, T.V., Triozzi, P.L., and Ponnazhagan, S. (2006). Enhanced transduction of mouse bone marrow-derived dendritic cells by repetitive infection with self-complementary adeno-associated virus 6 combined with immunostimulatory ligands. Gene Ther. *13*, 29–39.

35. Ussher, J.E., and Taylor, J.A. (2010). Optimized transduction of human monocyte-derived dendritic cells by recombinant adeno-associated virus serotype 6. Hum. Gene Ther. *21*, 1675–1686.

36. Aslanidi, G.V., Rivers, A.E., Ortiz, L., Song, L., Ling, C., Govindasamy, L., Van Vliet, K., Tan, M., Agbandje-McKenna, M., and Srivastava, A. (2013). Optimization of the capsid of recombinant adeno-associated virus 2 (AAV2) vectors: the final threshold? PLoS ONE *8*, e59142.

37. Chen, M., Maeng, K., Nawab, A., Francois, R.A., Bray, J.K., Reinhard, M.K., Boye, S.L., Hauswirth, W.W., Kaye, F.J., Aslanidi, G., et al. (2017). Efficient gene delivery and expression in pancreas and pancreatic tumors by capsid-optimized AAV8 vectors. Hum. Gene Ther. Methods *28*, 49–59.

38. Kay, C.N., Ryals, R.C., Aslanidi, G.V., Min, S.H., Ruan, Q., Sun, J., Dyka, F.M., Kasuga, D., Ayala, A.E., Van Vliet, K., et al. (2013). Targeting photoreceptors via intravitreal delivery using novel, capsid-mutated AAV vectors. PLoS ONE *8*, e62097.

39. Rosario, A.M., Cruz, P.E., Ceballos-Diaz, C., Strickland, M.R., Siemienski, Z., Pardo, M., Schob, K.L., Li, A., Aslanidi, G.V., Srivastava, A., et al. (2016). Microglia-specific targeting by novel capsid-modified AAV6 vectors. Mol. Ther. Methods Clin. Dev. *3*, 16026.

40. McCarty, D.M. (2008). Self-complementary AAV vectors; advances and applications. Mol. Ther. *16*, 1648–1656.

41. Shin, O., Kim, S.J., Lee, W.I., Kim, J.Y., and Lee, H. (2008). Effective transduction by self-complementary adeno-associated viruses of human dendritic cells with no alteration of their natural characteristics. J. Gene Med. *10*, 762–769.

42. Martino, A.T., Suzuki, M., Markusic, D.M., Zolotukhin, I., Ryals, R.C., Moghimi, B., Ertl, H.C., Muruve, D.A., Lee, B., and Herzog, R.W. (2011). The genome of self-complementary adeno-associated viral vectors increases Toll-like receptor 9-dependent innate immune responses in the liver. Blood *117*, 6459–6468.

43. Xin, K.-Q., Urabe, M., Yang, J., Nomiyama, K., Mizukami, H., Hamajima, K., Nomiyama, H., Saito, T., Imai, M., Monahan, J., et al. (2001). A novel recombinant adeno-associated virus vaccine induces a long-term humoral immune response to human immunodeficiency virus. Hum. Gene Ther. *12*, 1047–1061.

44. Weiner, L.M., Murray, J.C., and Shuptrine, C.W. (2012). Antibody-based immunotherapy of cancer. Cell *148*, 1081–1084.

45. Weiskopf, K., and Weissman, I.L. (2015). Macrophages are critical effectors of antibody therapies for cancer. MAbs *7*, 303–310.

46. Grommé, M., Uytdehaag, F.G.C.M., Janssen, H., Calafat, J., van Binnendijk, R.S., Kenter, M.J.H., Tulp, A., Verwoerd, D., and Neefjes, J. (1999). Recycling MHC class I molecules and endosomal peptide loading. Proc. Natl. Acad. Sci. USA *96*, 10326–10331.

47. Kurts, C., Robinson, B.W.S., and Knolle, P.A. (2010). Cross-priming in health and disease. Nat. Rev. Immunol. *10*, 403–414.

48. Sei, J.J., Haskett, S., Kaminsky, L.W., Lin, E., Truckenmiller, M.E., Bellone, C.J., Buller, R.M., and Norbury, C.C. (2015). Peptide-MHC-I from endogenous antigen outnumber those from exogenous antigen, irrespective of APC phenotype or activation. PLoS Pathog. *11*, e1004941.

49. Accolla, R.S., and Tosi, G. (2012). Optimal MHC-II-restricted tumor antigen presentation to CD4+ T helper cells: the key issue for development of anti-tumor vaccines. J. Transl. Med. *10*, 154.

50. Hung, K., Hayashi, R., Lafond-Walker, A., Lowenstein, C., Pardoll, D., and Levitsky, H. (1998). The central role of CD4(+) T cells in the antitumor immune response. J. Exp. Med. *188*, 2357–2368.

51. Borst, J., Ahrends, T., Bąbała, N., Melief, C.J.M., and Kastenmüller, W. (2018). CD4+ T cell help in cancer immunology and immunotherapy. Nat. Rev. Immunol. *18*, 635–647.

52. Castellino, F., and Germain, R.N. (2006). Cooperation between CD4+ and CD8+ T cells: when, where, and how. Annu. Rev. Immunol. *24*, 519–540.

53. Wong, S.B.J., Bos, R., and Sherman, L.A. (2008). Tumor-specific CD4+ T cells render the tumor environment permissive for infiltration by low-avidity CD8+ T cells. J. Immunol. *180*, 3122–3131.

54. Janssen, E.M., Lemmens, E.E., Wolfe, T., Christen, U., von Herrath, M.G., and Schoenberger, S.P. (2003). CD4+ T cells are required for secondary expansion and memory in CD8+ T lymphocytes. Nature *421*, 852–856.

55. Shedlock, D.J., and Shen, H. (2003). Requirement for CD4 T cell help in generating functional CD8 T cell memory. Science *300*, 337–339.

56. Janssen, E.M., Droin, N.M., Lemmens, E.E., Pinkoski, M.J., Bensinger, S.J., Ehst, B.D., Griffith, T.S., Green, D.R., and Schoenberger, S.P. (2005). CD4+ T-cell help controls CD8+ T-cell memory via TRAIL-mediated activation-induced cell death. Nature *434*, 88–93.

57. Sun, J.C., and Bevan, M.J. (2003). Defective CD8 T cell memory following acute infection without CD4 T cell help. Science *300*, 339–342.

58. Kang, T.H., Lee, J.H., Bae, H.C., Noh, K.H., Kim, J.H., Song, C.K., Shin, B.C., Hung, C.F., Wu, T.C., Park, J.S., and Kim, T.W. (2006). Enhancement of dendritic cell-based vaccine potency by targeting antigen to endosomal/lysosomal compartments. Immunol. Lett. *106*, 126–134.

59. Wu, T.C., Guarnieri, F.G., Staveley-O'Carroll, K.F., Viscidi, R.P., Levitsky, H.I., Hedrick, L., Cho, K.R., August, J.T., and Pardoll, D.M. (1995). Engineering an intracellular pathway for major histocompatibility complex class II presentation of antigens. Proc. Natl. Acad. Sci. USA *92*, 11671–11675.

60. Rowell, J.F., Ruff, A.L., Guarnieri, F.G., Staveley-O'Carroll, K., Lin, X., Tang, J., August, J.T., and Siliciano, R.F. (1995). Lysosome-associated membrane protein-1-mediated targeting of the HIV-1 envelope protein to an endosomal/lysosomal compartment enhances its presentation to MHC class II-restricted T cells. J. Immunol. *155*, 1818–1828.

61. Sanderson, S., Frauwirth, K., and Shastri, N. (1995). Expression of endogenous peptide-major histocompatibility complex class II complexes derived from invariant chain-antigen fusion proteins. Proc. Natl. Acad. Sci. USA *92*, 7217–7221.

62. Kreiter, S., Selmi, A., Diken, M., Sebastian, M., Osterloh, P., Schild, H., Huber, C., Türeci, O., and Sahin, U. (2008). Increased antigen presentation efficiency by coupling antigens to MHC class I trafficking signals. J. Immunol. *180*, 309–318.

63. Hunder, N.N., Wallen, H., Cao, J., Hendricks, D.W., Reilly, J.Z., Rodmyre, R., Jungbluth, A., Gnjatic, S., Thompson, J.A., and Yee, C. (2008). Treatment of metastatic melanoma with autologous CD4+ T cells against NY-ESO-1. N. Engl. J. Med. *358*, 2698–2703.

64. Marques, E.T.A., Jr., Chikhlikar, P., de Arruda, L.B., Leao, I.C., Lu, Y., Wong, J., Chen, J.S., Byrne, B., and August, J.T. (2003). HIV-1 p55Gag encoded in the lysosome-associated membrane protein-1 as a DNA plasmid vaccine chimera is highly expressed, traffics to the major histocompatibility class II compartment, and elicits enhanced immune responses. J. Biol. Chem. *278*, 37926–37936.

65. Lizée, G., Basha, G., Tiong, J., Julien, J.-P., Tian, M., Biron, K.E., and Jefferies, W.A. (2003). Control of dendritic cell cross-presentation by the major histocompatibility complex class I cytoplasmic domain. Nat. Immunol. *4*, 1065–1073.

66. Wherry, E.J., and Kurachi, M. (2015). Molecular and cellular insights into T cell exhaustion. Nat. Rev. Immunol. *15*, 486–499.

67. Hawkins, W.G., Gold, J.S., Dyall, R., Wolchok, J.D., Hoos, A., Bowne, W.B., Srinivasan, R., Houghton, A.N., and Lewis, J.J. (2000). Immunization with DNA coding for gp100 results in CD4 T-cell independent antitumor immunity. Surgery *128*, 273–280.

68. Bergman, P.J., McKnight, J., Novosad, A., Charney, S., Farrelly, J., Craft, D., Wulderk, M., Jeffers, Y., Sadelain, M., Hohenhaus, A.E., et al. (2003). Long-term survival of dogs with advanced malignant melanoma after DNA vaccination with xenogeneic human tyrosinase: a phase I trial. Clin. Cancer Res. *9*, 1284–1290.

69. Krotova, K., Marek, G.W., Wang, R.L., Aslanidi, G., Hoffman, B.E., Khodayari, N., Rouhani, F.N., and Brantly, M.L. (2017). Alpha-1 antitrypsin-deficient macrophages have increased matriptase-mediated proteolytic activity. Am. J. Respir. Cell Mol. Biol. *57*, 238–247.

70. Riaz, M., Raz, Y., Moloney, E.B., van Putten, M., Krom, Y.D., van der Maarel, S.M., Verhaagen, J., and Raz, V. (2015). Differential myofiber-type transduction preference of adeno-associated virus serotypes 6 and 9. Skelet. Muscle *5*, 37.

71. Lin, J., Zhi, Y., Mays, L., and Wilson, J.M. (2007). Vaccines based on novel adeno-associated virus vectors elicit aberrant CD8+ T-cell responses in mice. J. Virol. *81*, 11840–11849.

72. Zhu, F., Chen, T., Zhang, Y., Sun, H., Cao, H., Lu, J., Zhao, L., and Li, G. (2015). A novel adeno-associated virus-based genetic vaccine encoding the hepatitis C virus NS3/4 protein exhibits immunogenic properties in mice superior to those of an NS3-protein-based vaccine. PLoS ONE *10*, e0142349.

73. Jensen, S.M., Twitty, C.G., Maston, L.D., Antony, P.A., Lim, M., Hu, H.-M., Petrausch, U., Restifo, N.P., and Fox, B.A. (2012). Increased frequency of suppressive regulatory T cells and T cell-mediated antigen loss results in murine melanoma recurrence. J. Immunol. *189*, 767–776.

74. Olson, B.M., and McNeel, D.G. (2012). Antigen loss and tumor-mediated immunosuppression facilitate tumor recurrence. Expert Rev. Vaccines *11*, 1315–1317.

75. Sotillo, E., Barrett, D.M., Black, K.L., Bagashev, A., Oldridge, D., Wu, G., Sussman, R., Lanauze, C., Ruella, M., Gazzara, M.R., et al. (2015). Convergence of acquired mutations and alternative splicing of CD19 enables resistance to CART-19 immunotherapy. Cancer Discov. *5*, 1282–1295.

76. Gajewski, T.F. (2007). Failure at the effector phase: immune barriers at the level of the melanoma tumor microenvironment. Clin. Cancer Res. *13*, 5256–5261.

77. Freeman, G.J., Long, A.J., Iwai, Y., Bourque, K., Chernova, T., Nishimura, H., Fitz, L.J., Malenkovich, N., Okazaki, T., Byrne, M.C., et al. (2000). Engagement of the PD-1 immunoinhibitory receptor by a novel B7 family member leads to negative regulation of lymphocyte activation. J. Exp. Med. *192*, 1027–1034.

78. Blank, C., Gajewski, T.F., and Mackensen, A. (2005). Interaction of PD-L1 on tumor cells with PD-1 on tumor-specific T cells as a mechanism of immune evasion: implications for tumor immunotherapy. Cancer Immunol. Immunother. *54*, 307–314.

79. Curran, M.A., Montalvo, W., Yagita, H., and Allison, J.P. (2010). PD-1 and CTLA-4 combination blockade expands infiltrating T cells and reduces regulatory T and myeloid cells within B16 melanoma tumors. Proc. Natl. Acad. Sci. USA *107*, 4275–4280.

80. Pan, D., Kobayashi, A., Jiang, P., Ferrari de Andrade, L., Tay, R.E., Luoma, A.M., Tsoucas, D., Qiu, X., Lim, K., Rao, P., et al. (2018). A major chromatin regulator determines resistance of tumor cells to T cell-mediated killing. Science *359*, 770–775.

81. Strandt, H., Pinheiro, D.F., Kaplan, D.H., Wirth, D., Gratz, I.K., Hammerl, P., Thalhamer, J., and Stoecklinger, A. (2017). Neoantigen expression in steady-state Langerhans cells induces CTL tolerance. J. Immunol. *199*, 1626–1634.

82. Byers, A.M., Kemball, C.C., Moser, J.M., and Lukacher, A.E. (2003). Cutting edge: rapid in vivo CTL activity by polyoma virus-specific effector and memory CD8+ T cells. J. Immunol. *171*, 17–21.

83. Fridman, R., Benton, G., Aranoutova, I., Kleinman, H.K., and Bonfil, R.D. (2012). Increased initiation and growth of tumor cell lines, cancer stem cells and biopsy material in mice using basement membrane matrix protein (Cultrex or Matrigel) co-injection. Nat. Protoc. *7*, 1138–1144.